Journal of Engineering Sciences, Assiut University, Vol. 35, No. 3 pp. 645-663, May 2007

STRUCTURAL PERFORMANCE OF CONCRETE BEAMS REINFORCED WITH CFRP RODS OR HYBRID REINFORCEMENT

Hosny M. Soghair; Mahmoud H. Ahmed; Mohamed M. Ahmed
Civil Engineering Department, Faculty of Engineering, Assiut University, Assiut, Egypt
Zakaria H. Awadallah
Civil Engineering Department, Faculty of Engineering, AL-AZHAR University, Qena, Egypt

(Received April 8, 2007 Accepted May 3, 2007)

*Fiber Reinforced Polymer (FRP) rods; such as Carbon Fiber Reinforced Polymer rods (**CFRP**), are becoming the new wave of the future as a main reinforcement in concrete structures. Beams reinforced with this reinforcement had a reduction in ductility and stiffness. To improve the structural performance of such beams **hybrid** reinforcement; i.e. a combination of steel bars and **CFRP** rods have been proposed. This experimental study aims to throw a light on the flexural behavior of concrete beams reinforced with **CFRP** rods only and **hybrid** reinforcement. Eighteen concrete beams reinforced with different types and ratios of reinforcement (steel bars, **CFRP** rods or **hybrid**) were tested under mid span load up to failure. Pattern, width and spacing of cracks, modes of failure were observed, cracking and ultimate loads were recorded, deflections, and strains were measured. A comprehensive discussion for the obtained results was undertaken. Cracking load, ultimate load, mid span deflection and crack width for the tested beams were also theoretically predicted. A comparison between the predicted values with the corresponding experimental results was also given. An adequate level of ductility and stiffness in **hybrid** reinforced members was observed. Finally the conclusions and recommendations that are useful for the structural engineers in this concern are drawn.*

KEYWORDS: *R.C beams; FRP rods; Carbon Fiber Rods; Deflection; Cracking; Ductility; Hybrid Reinforcement.*

NOTATION

A_t = area of tension reinforcement.
A_s = area of steel reinforcement.
A_f = area of FRP reinforcement.
A^* = concrete area surrounding one bar.
d_c= concrete cover from the center bar.
d_S = depth from top fiber to steel bar.
d_f = depth from top fiber to FRP rod.
E_c= modulus of elasticity of concrete.
I_{Cr} = cracked moment of inertia.
I_e = effective moment of inertia.
P_{Cr} = cracking load.
P_U = ultimate load.
w_{max} = maximum crack width.
ε_s= tensile steel strain.
ε_{CFRP} = tensile strain in CFRP rods.
μ = steel reinforced ratio = (A_S/A_f)

E_f = modulus of elasticity of FRP rods.	ρ = reinforcement ratio.
E_s = modulus of elasticity of steel bars.	Δ_{max} = maximum deflection.
f_f = FRP stress.	ω = the tension force index ratio
f_s = steel stress.	$= \frac{\Sigma A_S \, d_S \, f_y}{\Sigma A_S \, d_S \, f_y + \Sigma A_f \, d_f \, f_f}$.
M_a = applied moment.	
M_{Cr} = cracking moment.	
I_g = uncracked moment of inertia.	d_b = bar diameter.

1. INTRODUCTION

R.C. structures subjected to aggressive environments are affected by the corrosion of reinforcing steel bars, concrete deterioration and loss of serviceability. This led to the attempt of using FPR rods as a main reinforcement in lieu of steel bars. FRP rods have a resistance to corrosion, lightweight, high tensile strength, electromagnetic resistance, and high fatigue endurance. However, the low modulus of elasticity, low transverse strength, low bond to concrete cause high deformability of structural elements and large crack width. Another concern designers have when using FRP rods in concrete flexural members is the linear elastic behavior up to failure without yielding, therefore leading to sudden collapse in a brittle manner. So, some alternative solutions have been proposed, such as the use of **hybrid** reinforcement; i.e. a combination of steel bars and **CFRP** rods which takes advantages from both materials, in particular, the introduction of **CFRP** rods increases the durability and the ultimate capacity of members, while steel reinforcement improves the structural performance in terms of stiffness and ductility. The effectiveness of this new reinforcing system remains problematic and continued research is needed [11], [13].

Factors such as type of fiber, resin, fiber volumetric ratio and orientation, dimensional effects, rate of curing, quality control, and manufacturing process have a significant effect on the mechanical characteristics of the FRP rods. So variations will occur in rods with various fibers volume fractions, even in rod with the same diameter, appearance, and constituents. FRP rods have a lower bond strength and higher slip at failure than conventional steel reinforcement. When the concrete cover is less than $2d_b$ splitting failure can occur. The bond strength of FRP rods does not depend on the value of concrete strength, as far as the concrete strength is greater than 30 MPa because the bond failure interface happens in the surface of FRP rod. However, for lower concrete strengths the failure takes place in the concrete matrix and the bond behavior of the rod is directly related to the bond strength [1], [6].

Beams reinforced with **GFRP** rods only with lower strength failed with a bond slippage of **GFRP** rods, while the beams reinforced with hybrid reinforcement indicated a concrete crushing failure type. With increasing in the number of **GFRP** rods, lower strength concrete beam failed with concrete crushing and concrete splitting at the steel bars level, but with higher concrete strength, flexural failure mode with diagonal shear cracks at its shear span were occurred [9], [11].

Deflection is dependent on the sectional flexural stiffness, the reinforcement ratio and modulus of elasticity for FRP rods. The deflection of the **GFRP** R.C beams is higher than those of the steel R.C beams, deflection continued to increase with increasing the load, thereby exhibiting some ductility. Deflection reduces with

increasing reinforcement ratio, but very high **GFRP** reinforcement ratios are required to make the deflection within that range comparable to steel bars. The beams reinforced with **GFRP** rods owing to their lower elastic modulus exhibit a reduced in stiffness than those reinforced with **CFRP** rods [14], [15].

The cracks in the **GFRP** reinforced specimens initiated suddenly and were larger than the corresponding cracks in steel reinforced beams. Two modes of flexural failure can be distinguished; by concrete compressive crushing in over reinforced beam or sudden rupture of FRP rods for under reinforced beam. Over reinforcement of the section took advantage of the ductility inherent in concrete itself to produce reserve capacity after reaching ultimate load. Reductions in cracks width beside an increase in cracks number have been observed when FRP rods were combined with steel bars [4], [13].

2. EXPERIMENTAL WORK

2.1. Materials:

Local natural sand, well-graded basalt with nominal size of 20 mm, Ordinary Portland cement, additives as Silica fume and Addicrete BVF were used. CFRP rods of 100cm length and 12mm diameter were used as a main reinforcement in middle part of the span, and then each was replaced by 3φ12 steel bars at the beam-ends, through lap splice. The mechanical properties of CFRP rods given by the manufacturer were:

Table (1): The details of the tested beams

Spec.	a/d	Type of Reinf.	Main Reinf. (mm)	ρ(%) =[A_t/b*d]	ω %	Upper.Reinf. (mm)
A_1	2.9	Steel	$2S_{16}$	1.48	1	2Φ10
A_2	2.9	Steel	$2S_{16}$ + $4S_4$	1.94	1	2Φ10
A_3	2.9	Steel	$4S_{16}$ + $4S_4$	3.44	1	2Φ10
B_1	2.9	CFRP	$1C_{12}$	0.378	1	2Φ10
B_2	2.9	Hybrid	$1C_{12}$ + $6S_4$	1.12	7.32	2Φ10
B_3	2.9	Hybrid	$2C_{12}$ + $4S_4$	1.3	10.13	2Φ10
C_0	4.4	Steel	$4S_{16}$ + $2S_6$	3.19	1	2Φ10
C_1	4.4	Steel	$4S_{16}$ +$2S_{10}$+$2S_6$	3.77	1	2Φ10
C_2	4.4	Steel	$4S_{16}$ +$2S_{12}$+$2S_6$	4.023	1	3Φ10
C_3	4.4	Steel	$4S_{16}$+$4S_{10}$	4.14	1	3Φ10
C_4	4.4	Steel	$6S_{16}$	4.47	1	3Φ10
C_5	4.4	Steel	$4S_{16}$ +$4S_{12}$	4.65	1	3Φ10
D_0	4.4	Hybrid	$1C_{12}$ + $6S_6$	1.044	4.1	2Φ10
D_1	4.4	Hybrid	$1C_{12}$ + $2S_{10}$ +$4S_6$	1.418	8.06	3Φ10
D_2	4.4	Hybrid	$1C_{12}$ + $2S_{12}$ +	1.67	12.5	1Φ10+2Φ12
D_3	4.4	Hybrid	$1C_{12}$ + $4S_{10}$+ $2S_6$	1.79	13.9	1Φ10+2Φ12
D_4	4.4	Hybrid	$1C_{12}$ + $2S_{16}$ +	2.16	16.5	3Φ12
D_5	4.4	Hybrid	$1C_{12}$ + $4S_{12}$+ $2S_6$	2.3	17.9	3Φ12

Where : C = CFRP rods, S = Steel bars, Hybrid = (CFRP rods + Steel bars).

tensile strength 2300 MP_a, modulus of elasticity 130 GP_a and ultimate deformation (1.8 %). High tensile steel bars of (**4, 10, 12, and 16**) mm were used as a longitudinal reinforcement, while mild steel bars of (**6**) mm diameter were used for stirrups or as a longitudinal bars in tension zone. All beams had the same cross section dimension of (**15 x 20**) cm with different in shear span to depth ratio (**a/d**) as shown in Table (1), Fig. (1).

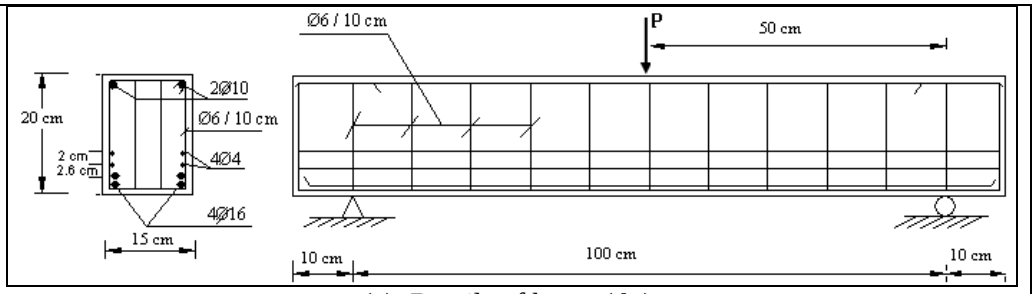

(a): Details of beam (**A_3**).

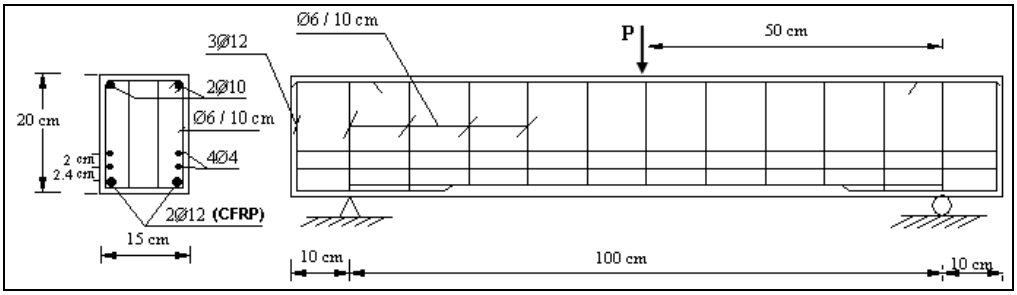

(b): Details of beam (**B_3**).

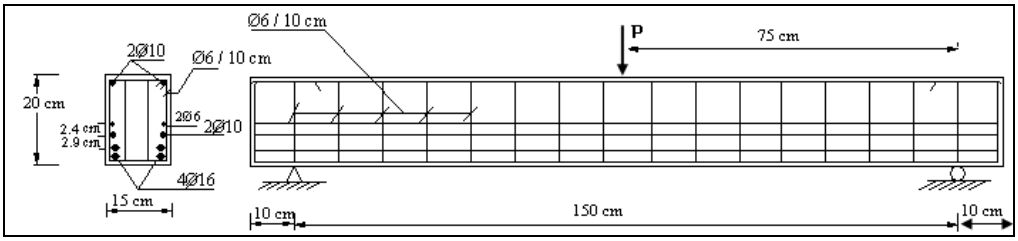

(c): Details of beam (**C_1**).

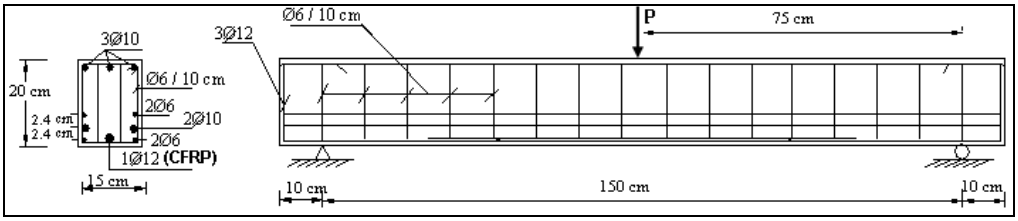

(d): Details of beam (**D_1**).

Fig. (1): Details of some specimens used in experimental program.

2.2. Preparing Test Specimens and Test Procedure:

Mixing was performed using a concrete tilting drum mixture. The time of mixing was about five minutes. Clean steel forms were used. Their inner sides were coated with oil before casting. Concrete was placed and compacted mechanically by internal electrical vibrator. In the second day, the steel forms were removed and the daily curing was started up to the day before testing. All beams were simply supported and tested at 28 days age under mid-span static load using the available testing machine (EMS 60-Ton). The deflection of the tested beam was measured using dial gage having an accuracy of 0.001 inch. The induced strains in main steel and CFRP rods were measured by means of electrical strain gages. The concrete strength was about 550 k_g/cm^2. The load was applied in increments of 0.5t, and was kept constant between two successive increments for about five minutes to allow for reading of the strain and dial gages and marking the crack propagation.

3. EXPERIMENTAL RESULTS AND DISCUSSION

The cracks in both sides for all the tested beams are approximately similar. The first crack is initiated in the region of maximum moment zone as a vertical flexural crack nearly under the load point. With increasing the applied load another cracks formed and propagated from the bottom fiber of beam towards the application point, Fig. (2). Table (2) gives the final mode of failure for the tested beams.

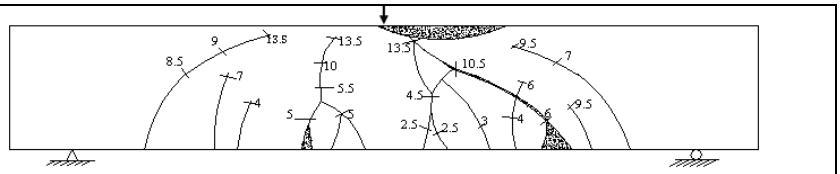

(a): Crack pattern for beam ($\mathbf{A_1}$).

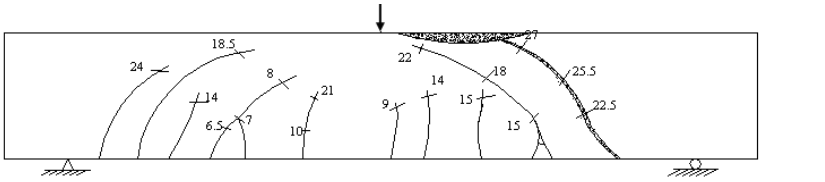

(b): Crack pattern for beam ($\mathbf{A_3}$).

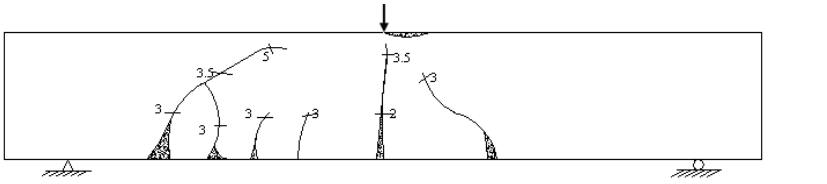

(c): Crack pattern for beam ($\mathbf{B_1}$).

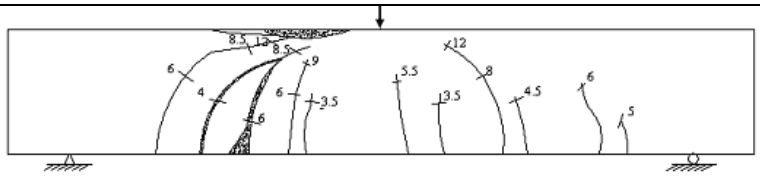

(d): Crack pattern for beam ($\mathbf{B_3}$).

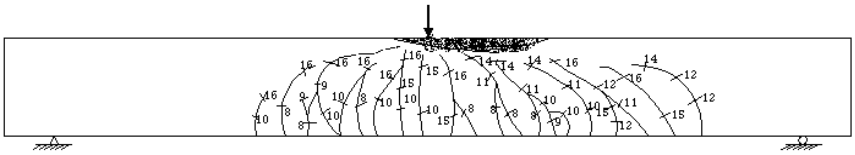

(e): Crack pattern for beam ($\mathbf{C_1}$).

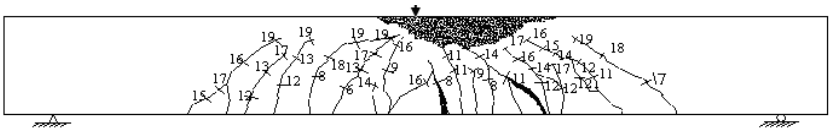

(f): Crack pattern for beam ($\mathbf{C_5}$).

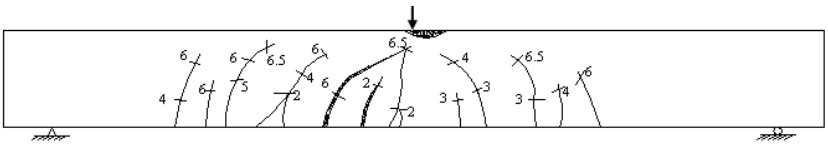

(g): Crack pattern for beam ($\mathbf{D_0}$).

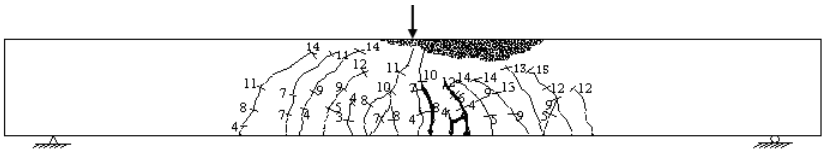

(h): Crack pattern for beam ($\mathbf{D_4}$).

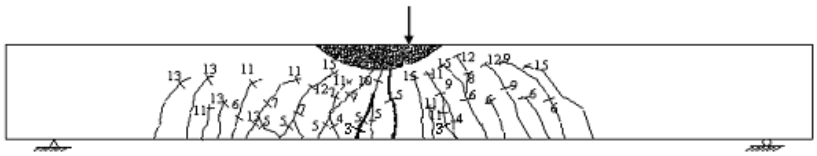

(i): Crack pattern for beam ($\mathbf{D_5}$).

Fig (2): Typical cracking pattern for some experimental beams.

Table (2): Test results for all tested groups.

Spec.	P_{Cr} (ton)	P_U (ton)	Max. ε_s	Max. ε_f	Max. Δ (mm)	Mode of Failure
A_1	2.5	14	0.01333	-	10.47	F - C
A_2	4.5	14	0.00841	-	10.12	F - C
A_3	6.5	28	0.00593	-	7.93	S - C
B_1	2	8.5	-	0.00513	10.5	L - D
B_2	3	8.5	-	0.00493	10.23	L - D
B_3	3.5	13.5	-	0.00475	9.73	L - D
C_0	6	15.7	0.00281	-	7.9	S - C
C_1	8	16.8	0.00277	-	8.08	S - C
C_2	11	17	0.00263	-	6.8	S - C
C_3	6	18.5	0.00290	-	10.9	S - C
C_4	9	19.1	0.00308	-	7.8	S - C
C_5	6	19.6	0.00291	-	8.0	S - C
D_0	2	7	-	0.00693	5.98	F - C
D_1	3	9	0.00310	0.00650	5.36	F - C
D_2	3	10.3	0.00290	0.00550	5.37	F - C with debonding
D_3	3	12	0.00285	0.00580	5.2	F - C with debonding
D_4	3	15	0.00298	0.00591	4.95	F - C
D_5	3	15.9	0.00271	0.00550	4.96	F - C

Where: F-C = Flexural–Compression**,** S-C = Shear–Compression, L-D = Local Dowel.

3.1. BEAMS WITH SHEAR SPAN TO DEPTH RATIO (a/d = 2.9).

3.1.1. Cracks Pattern and Modes of Failure:

The presence of CFRP rods in-group (**B**) led to decreasing the number of cracks, compared with beams reinforced with ordinary steel bars, group (**A)**. Therefore, the average crack spacing in-group (**B)** is more than that in-group (**A**), Fig. (3). This is from one hand due to the lower modulus of elasticity for CFRP rods than in steel bars, from the other hand due to the better distribution of tensile reinforcement in the tension zone in case of steel reinforced beams.

The increasing in CFRP rods ratio led to increasing the number of cracks and decreasing their width and spacing, beams (**B_1 and B_3**). The local dowel failure occurred in beams in group (**B**) due to the increasing in the critical crack width; the ultimate deformation capacity (**1.8) %** of the CFRP rod is locally reached causing high stress concentration at the level of CFRP rods and then the locally dowel action failure was happened. Photo (1) shows the final mode of failure for beam (**B_3).**

3.1.2. Maximum Induced Deformations:

The values of measured deflection and tensile strain in beams (**A_1, A_3, B_1** and **B_3**) decreased as the reinforcement ratio increased, Figs. (4) and (5). At any load level, these values are greater in beams (**B_1** and **B_3**) than those in beams (**A_1** and **A_3**); this can

be attributed to the lower modulus of elasticity for CFRP rods than in steel bars. It can be seen that the tensile strain in CFRP rods are nearly linear up to failure, while the yielding of steel bars are noticed.

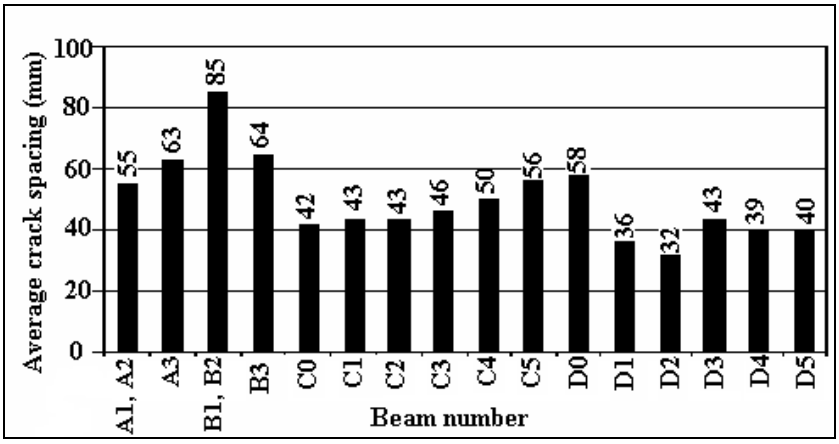

Fig. (3): Average crack spacing over the beam length.

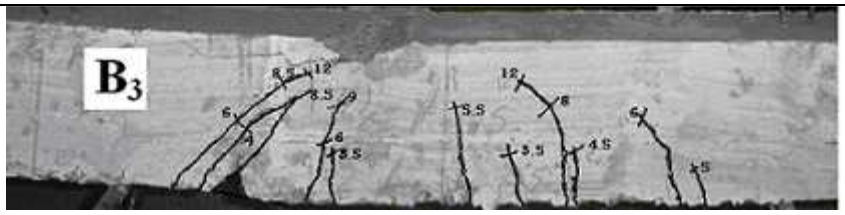

Photo. (1): Final failure mode of beam (B_3).

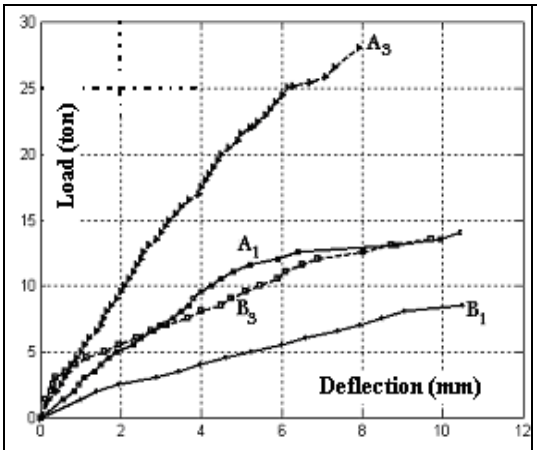

Fig. (4): Load – deflection for beams (A_1, B_1, A_3 and B_3).

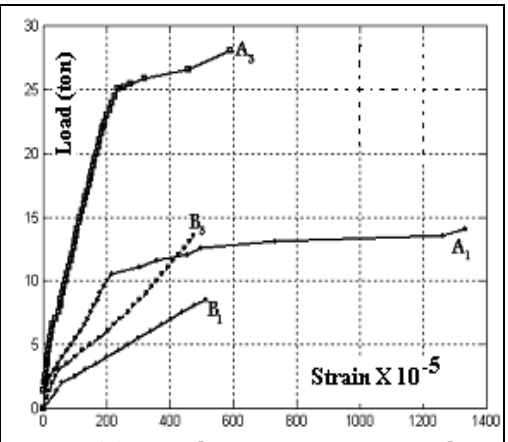

Fig. (5): Load – strain in CFRP rods and steel bars for beams (A_1, B_1, A_3 and B_3).

3.1.3. Cracking and Ultimate Loads:

The cracking and ultimate loads in CFRP beams ($\mathbf{B_1}$ and $\mathbf{B_3}$) are smaller than that in conventional R.C beams ($\mathbf{A_1}$ and $\mathbf{A_3}$). This can be attributed to the lower modulus of elasticity of CFRP rods than steel bars, which led to early appearance the cracks; in addition to that, concentration of the reinforcement in the tension side in beams ($\mathbf{B_1}$ and $\mathbf{B_3}$) led to decreased the number of cracks with wider cracks width, which from its side led to the early occurrence of dowel failure. Cracking and ultimate load are increased as the ratio of reinforcement increased, Table (2).

At failure, the maximum tensile force in the CFRP rods at maximum moment section is not fully utilized and was in the range of (**50 to 60**) % of their ultimate tensile force, because of the dowel action failure.

3.2. BEAMS WITH SHEAR SPAN TO DEPTH RATIO (a/d = 4.4).

3.2.1. Cracks Pattern and Modes of Failure.

The using of hybrid reinforcement as tension reinforcement in group (**D)** led to improvement in cracks pattern; the cracks propagated gradually, the number of cracks increased, crack width and spacing between cracks decreased and the distribution of cracks along the beam span were better than that in group (**B**), this is due to the better distribution of reinforcement in the tension zone. This improvement in crack appearance was more pronounced as the ratio of steel reinforcement ($\mu = A_s/A_f$) increased. In group (**D**), the using of hybrid reinforcement prevents the occurrence of local dowel failure.

In beams ($\mathbf{D_0}$ and $\mathbf{D_1}$) the mode of failure was flexure - compression, with increasing the amount of steel reinforcement in beam ($\mathbf{D_2}$ and $\mathbf{D_3}$) the propagation of the flexural cracks was relatively slower which led to an increase in the ultimate load; however the final failure was due to flexure-compression with debonding between CFRP rods and concrete. The debonding failure may be due to the small concrete cover for CFRP rods. A further increase in the amount of steel reinforcement, beam ($\mathbf{D_4}$ and $\mathbf{D_5}$) helped in delaying the propagation of the flexural cracks and hence preventing the debonding failure.

In the same time, it is clear that the number of cracks in group (**D**) were less than that in group (**C**) which reinforced with steel bars only, while the crack width in group (**D**) still grater than that in group (**C**); this is due to the yielding of steel bars in group (**D**), liner behavior of CFRP rods until failure and the debonding between CFRP rods and concrete. The critical crack width at failure decreased as the ratio of steel bars increased, Fig. (6). Photo (2, 3 and 4) shows the final mode of failure for beams ($\mathbf{D_1}$, $\mathbf{D_2}$ and $\mathbf{D_3}$).

3.2.2. Maximum Induced Deformations:

The load - deflection curves of beams in-group (**D**) reinforced with hybrid reinforcement become more flat and are still linear up to failure stage compared with that in-group (**C**), Fig. (7). From this curves it is appeared that an increase in deflection values occurred at any load level up to failure in beams reinforced with hybrid

reinforcement compared with that reinforced with steel bars only, especially after cracking stage. In the same time, it was observed that a relevant increase in stiffness for beams (**D_1** and **D_2**) with respect to the control beam, (**D_0**), which approach that in beam (**C_0**) with steel reinforced only. Also It is obvious that, the increasing in steel bars ratio led to increasing the stiffness and improving in load – deflection curves, Fig. (8).

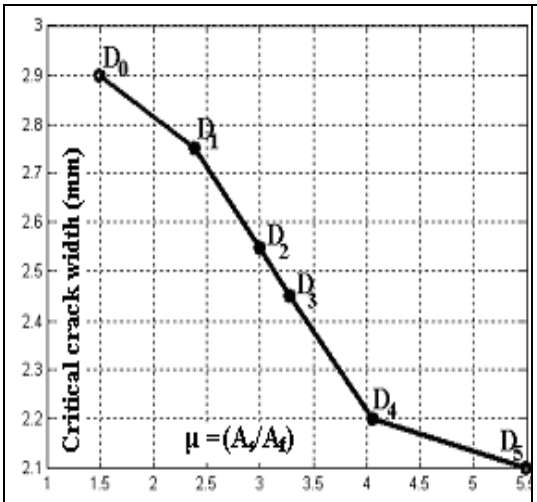

Fig. (6): Critical crack width versus "μ" for Group (D).

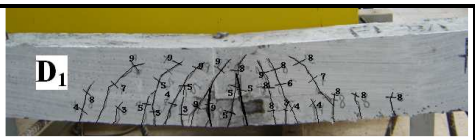

Photo. (2): Final failure mode of beam (D_1).

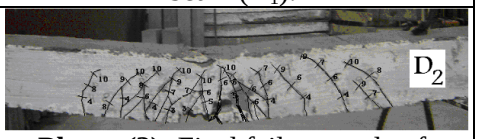

Photo. (3): Final failure mode of beam (D_2).

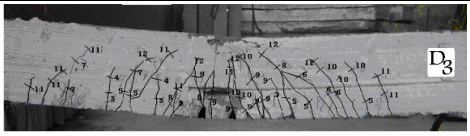

Photo. (4): Final failure mode of beam (D_3).

The measured value of mid span deflection at (**0.5 P_U**) and (**0.9 P_U**) is plotted against the steel ratio "**μ**" in Fig. (9). It can be observed that the values of (**$\Delta_{0.5}$ and $\Delta_{0.9}$**) decreased with increasing the steel bars ratio "**μ**". In addition the rate of this reduction in deflection was bigger for lower values of "**μ**" (**$\mu \leq 3.5$**), while an almost constant trend was obtained with a further increase in "**μ**". This result suggests the possibility of defining an optimal value of steel reinforcement ratio to limit the deformability of the beam. The same result was obtained in a previous work [13]. In spite of this decrease in (**$\Delta_{0.5}$ and $\Delta_{0.9}$**) an increase in the ratio of (**$\Delta_{0.9}/\Delta_{0.5}$**) was observed with increasing (**μ**) which indicate an improvement in the ductility of the beam, Fig. (10).

The maximum mid span deflection at failure were plotted against the tension force **index ratio "ω**" as shown in Fig. (11). It can be seen that the maximum mid span deflection decrease as the index ratio increased.

Figure (12) shows the relation between the induced deflection and the applied moment for beams with different (**a/d**) ratio. It can be seen that using of steel reinforcement with low modulus CFRP rods decreases the obtained mid span deflection at any load level and increased the ultimate moment.

The measured values of tensile steel strain in both beams in groups (**C** and **D**) had reached its yielding g value, while the strain in CFRP rods in group (**D**) still linear and were greater than the steel strain in the same beam reaching only about **40%** of their ultimate strain approximately, Fig. (13), Fig. (14). Depending on the amount of

steel reinforcement, the yielding of steel bars in-group (**D**) had occurred at the applied load less than that required to produce yielding in the corresponding beams in group (**C**). This may be attributed to the lower modulus of elasticity for CFRP rods than in steel bars, and the debonding between CFRP rods and concrete, which led to presence of large crack width and the excessive strains adjacent steel reinforcement in these cracks opening.

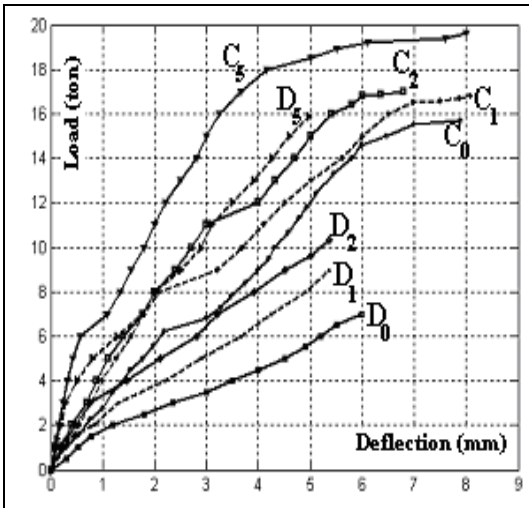

Fig. (7): Load – deflection for beams (C_0, D_0, C_1, D_1, C_2, D_2, C_5 and D_5).

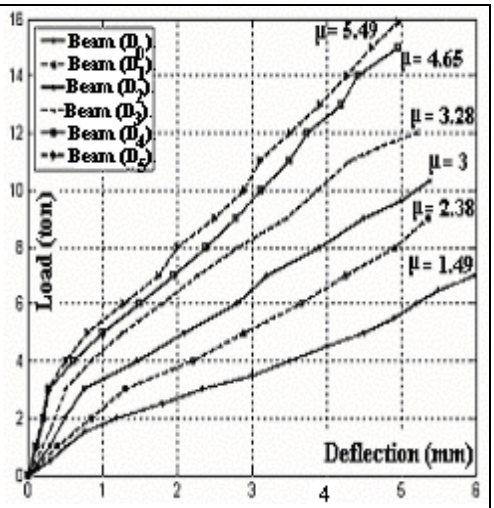

Fig. (8): Load – deflection curves varying "$\mu = (A_S/A_f)$" for group (D).

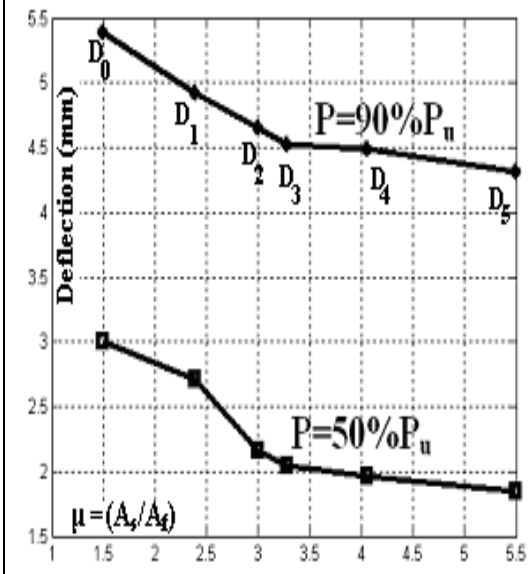

Fig. (9): Effect of steel bars ratio "μ" on mid span deflection values for group (D).

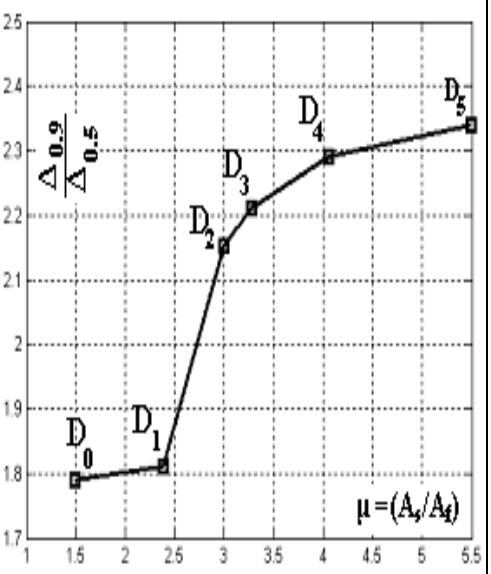

Fig. (10): Ductility values versus "μ". For group (D).

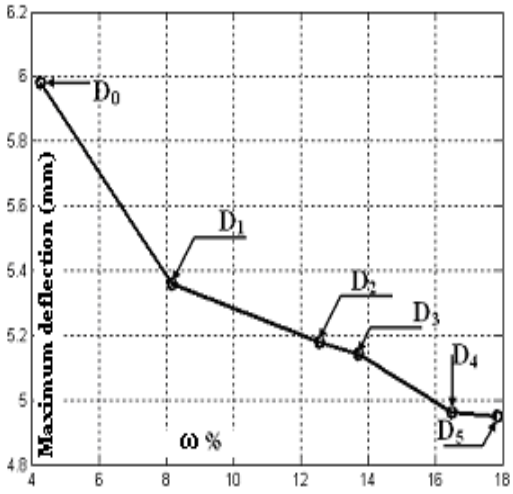

Fig. (11): Effect of "ω" on maximum mid span deflection for group (D).

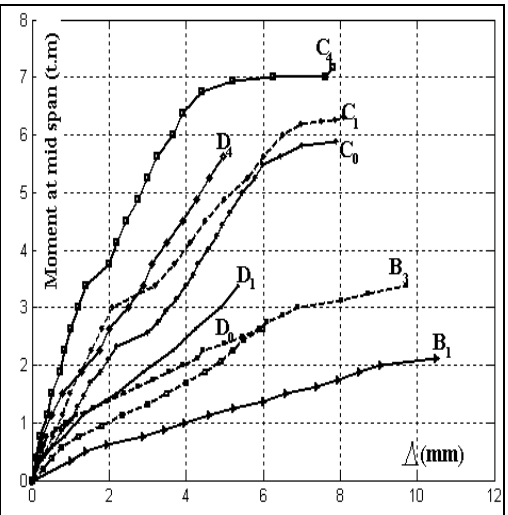

Fig. (12): Moment versus (Δ) for beams (C_0, D_0, C_1, D_1, C_4,, D_4, B_1 and B_3).

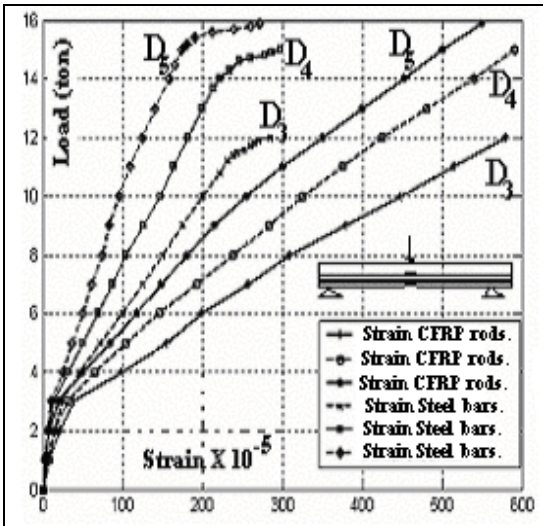

Fig. (13): Load – strain in CFRP rod and steel bars for beams (D_3, D_4 and D_5).

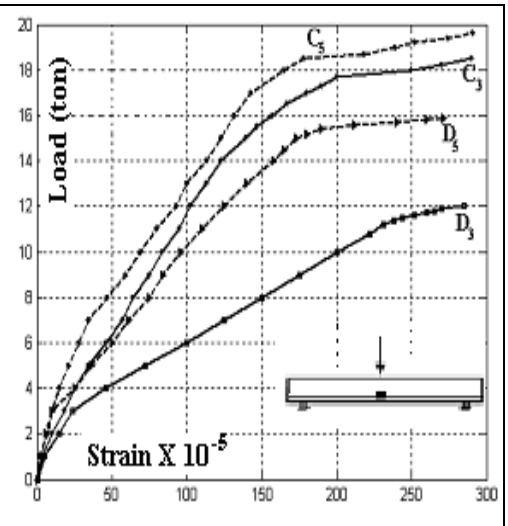

Fig. (14): Load – strain in steel bars for beams (C_3, D_3, C_5 and D_5).

3.2.3. Cracking and Ultimate Loads:

There was an enhancement in the ultimate load when using hybrid reinforcement, this enhancement is generally increased with increasing in steel bars ratio, Table (2), Fig. (15). Comparing with the beams in group (**C**), it was observed that the cracking and ultimate loads in group (**D**) were smaller than that in group (**C**), this due to the lower modulus of elasticity for CFRP rods than in steel bars which results in large deflection and higher crack widths and spacing.

The ultimate loads at failure for beams in group (**D**) having the same amount of CFRP reinforcement and variable amount of steel bars were plotted against the tension force index ratio "**ω**" as shown in Fig (16). From this figure, it is clear that the ultimate load increased as the index ratio increased.

The predicted values of ultimate loads were estimated using the analysis of cracked section and the compatibility of strain at failure, Fig (17). The predicted values of $\mathbf{P_U}$ for beams (**D_0, D_1, D_2 and D_3**) with relatively small amount of steel reinforcement were near the corresponding experimental values. The deviation between them was increased as the ratio "**μ**" increased. For beam (**D_3**) with **(μ=3.28%),** the maximum deviation of about 20%. This deviation reached about 45% in beams (**D_4 and D_5**).

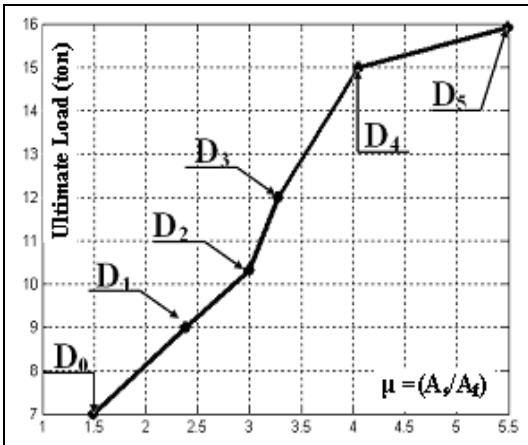

Fig. (15): Effect of "μ" on ultimate load for group (D).

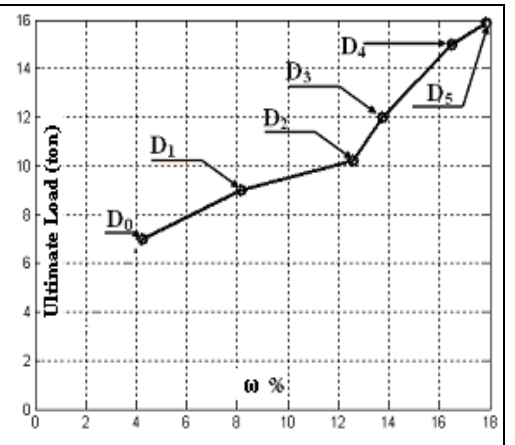

Fig. (16): Effect of "ω" on ultimate load for group (D).

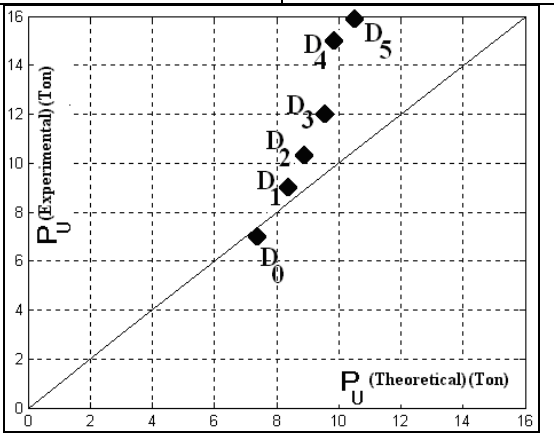

Fig. (17): Experimental and theoretical ultimate load for group (D).

4. COMARISON BETWEEN EXPERIMENTAL AND THEORETICAL RESULS.

4.1. Mid span deflection:

The following equation was used to calculate the mid span deflection Δ_{max} for the tested beams subjected to one centric concentrated load (**P**).

$$\Delta_{max} = \frac{P L^3}{48 E_c I_e} \quad (1)$$

Various methods are available for predicting the effective moment of inertia $\mathbf{I_e}$ in beams reinforced with FRP rods or with steel bars. These methods are given in Table (3).

Table (3): Predictive formulae for deflection

Approach	Formulae	
ACI-318.[2]	$I_e = \left(\frac{M_{Cr}}{M_a}\right)^3 B_d I_g + \left[1-\left(\frac{M_{Cr}}{M_a}\right)^3\right] I_{Cr} \subseteq I_g$	$B_d = 1$
ACI-440.IR.01.[3]		$B_d = \alpha_d \left[\frac{E_f}{E_s}+1\right]$ $\alpha_d = 0.5$
ISIS Canada.[10]	$I_e = \frac{I_g I_{Cr}}{I_{Cr} + \left[1-0.5\left(\frac{M_{Cr}}{M_a}\right)^2\right](I_g - I_{Cr})}$	
Charif Model.[7]	$I_e = \frac{I_g I_{Cr}}{I_{Cr}\zeta + 1.15 I_g (1-\zeta)}$, $\zeta = \frac{0.5 M_{Cr}}{M_a}$	
Hall et al.[8]	$I_e = \frac{I_g I_{Cr}}{\left[I_1 + B_1 B_2 \left(\frac{M_{Cr}}{M_a}\right)^2 (I_{Cr} - I_g)\right]}$	$B_1 = 0.5$ $B_2 = 0.8$
Benmokrane et al.[5]	$I_e = \alpha I_{Cr} + \left(\frac{I_g}{B} - \alpha I_{Cr}\right)\left(\frac{M_{Cr}}{M_a}\right)^3 \subseteq I_g$	$\alpha = 0.84$ $B = 7$
Masmoudi et al.[12]	$I_e = I_{Cr} + (\beta I_g - I_{Cr})\left(\frac{M_{Cr}}{M_a}\right)^3 \subseteq I_g$	$B = 0.6$

The calculated values of mid span deflections according to these equations were plotted against the corresponding loads for beams **(B_1, B_3, D_0, D_1, D_2, D_3, D_4 and D_5).** The corresponding experimental load-deflection curve was also included in the figure for the sake of comparison. It is clear from these figures that both of experimental and theoretical results give almost the same trend and shape for the load-deflection curves. The experimental values at failure were always greater than the predicted one in CFRP

reinforced beams, Fig (18, 19) and the nearst value from all the used equations was that proposed by Benmokrane with maximum deviation of about 20%. For hybrid reinforcement beams, the predicted equation by Benmokrane was a reasonable for beams (**D_0, D_1 and D_2**) with relatively small steel ratio with maximum deviation at failure of about 8%, Fig (20), while with higher steel ratio of beams (**D_3, D_4 and D_5**) the experimental values for mid span deflection were greater than that predicted by Benmokrane, Fig (21).

Fig (22) show that the experimental deflections values for beam (D_3) are well with those predicted by ACI 440.1R.01.

This indicates that we need to adjust new equation for estimating the mid span deflection for this type of reinforcement especially when using high percentage of steel and CFRP reinforcement.

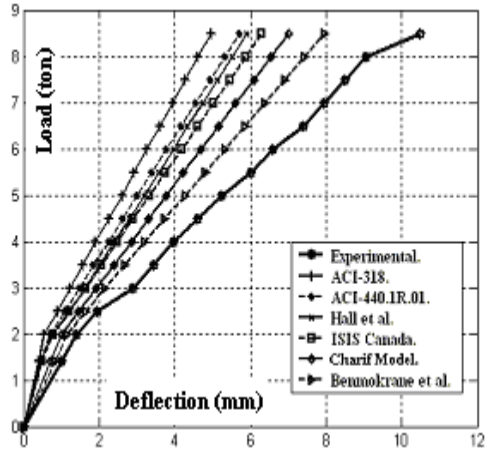

Fig. (18): Experimental and theoretical deflection of beam (B_1).

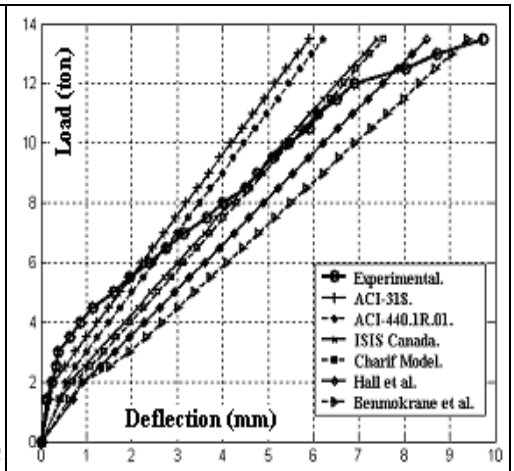

Fig. (19): Experimental and theoretical deflection of beam (B_3).

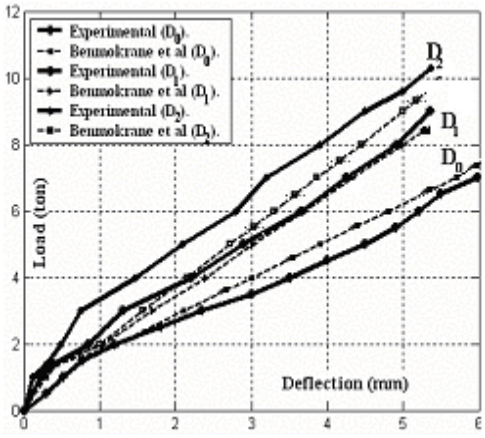

Fig. (20): Experimental mid span deflection and those predicted by Benmokrane for beams (D_0, D_1, and D_2).

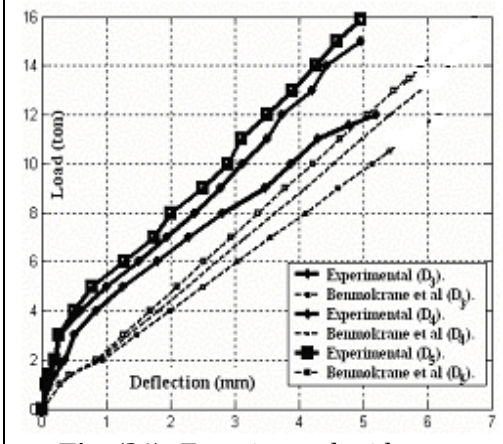

Fig. (21): Experimental mid span deflection and those predicted by Benmokrane for beams (D_3, D_4, and D_5).

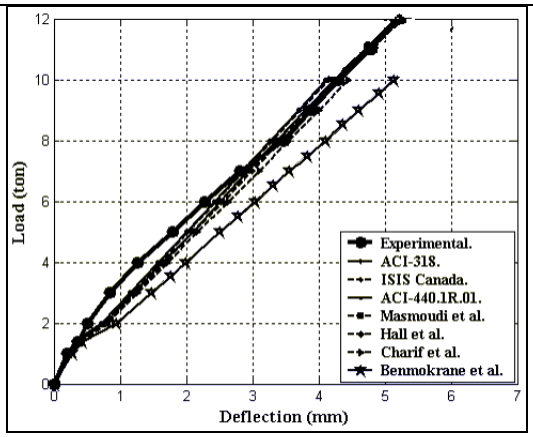

Fig. (22): Experimental and theoretical deflection of beam (D_3).

4.2. Crack width:

ACI 440.1R-01 [3] offers the following expressions to calculate crack widths *w* in beams reinforced with FRP rods only:

$$W = \frac{2.2}{E_f} B K_b f_f \sqrt[3]{(d_c A^*)} \quad (2)$$

For hybrid reinforcement we used the following expressions:

$$W = 2.2 B K_b \left[\frac{f_f}{E_f} + \frac{f_s}{E_s} \right] \sqrt[3]{(d_c A^*)} \quad (3)$$

The comparison between experimental and theoretical of maximum crack width for beams in group (**D**) indicates that the crack width are always smaller than the experimental of critical crack width at failure, Table (4).

Table (4) Comparison between experimental and theoretical of maximum crack width

Spec.	Experimental	Theoretical	Failur mode
	w_{max} (mm)	w_{max} (mm)	
D_0	2.9	1.45	F - C
D_1	2.75	1.64	F - C
D_2	2.55	1.65	F - C With debonding
D_3	2.45	1.61	F - C With debonding
D_4	2.2	1.54	F - C
D_5	2.1	1.52	F - C

CONCLUSIONS

Based on the analysis and discussion of the experimental and theoretical results given above, the following conclusions can be drawn:

1. The combination of steel bars and CFRP rods takes advantages from both materials. In particular, the introduction of CFRP rods increases the durability of structural elements and the ultimate capacity, while steel reinforcement improves the structural performance in terms of stiffness and ductility.
2. Beams reinforced with CFRP rods only show a reduction in stiffness than beams reinforced with hybrid reinforcement or with that reinforced with conventional steel bars only.
3. Deflection behavior of concrete beams reinforced with CFRP rods only or with hybrid reinforcement and subjected to bending moment was linearly before and after cracking.
4. Crack width, spacing between cracks and the deformations of concrete member reinforced with CFRP rods only were larger than that reinforced with hybrid reinforcement or with conventional steel bars only. This due to the low elastic modulus of CFRP rods to steel bars, different bond characteristics CFRP reinforcement.
5. Bond properties of CFRP rods and the interaction between CFRP rods and the concrete are essential for the structural analysis. Consequently, bond tests should be considered as fundamental for the mechanical characterization of CFRP rods, like tensile tests.
6. Cracking and ultimate loads in CFRP or hybrid reinforced beams are smaller than that in conventional R.C. beams. This can be attributed to the lower modulus of elasticity of CFRP rods than steel bars.
7. The using of hybrid reinforcement as tension reinforcement especially with high steel ratio led to improvement in crack patterns; the cracks propagated gradually, the number of cracks increased, crack width and spacing between cracks decreased and the distribution of cracks along the beam span were better than that reinforced with CFRP only or that with lower steel ratio, this is due to the better distribution of reinforcement in the tension zone.
8. Deflections estimated according to Benmokrane are in good agreement with the experimental results for beams reinforced with hybrid reinforcement with small ratios of steel reinforcement, while the equation proposed by ACI 318 can be used for higher ratios of steel.
9. More studies are needed to verify the experimental and predictive model for concrete beams reinforced with different types of FRP rods or with hybrid reinforcement.

REFERENCES

[1] Achillides Z., and Pilakoutas K. (2004), “Bond Behaviour of Fibre Reinforced Polymer Bars under Direct Pullout Conditions,” Journal of Composites for Construction, ASCE, Vol. 8, No. 2, April 2004, pp. 173-181.

[2] ACI Committee 318, "Building Code Requirements for Structural Concrete (ACI 318-02) and Commentary (318R-95) "American Concrete Institute, Farmington Hills, Mich., 1995, 369 pp.

[3] ACI Committee 440.1R.01,"Guide for the design and construction of concrete reinforced with FRP bars", American Concrete Institute, 2001. 97 pp.

[4] Alsayed, S. H., Almusallam, T. H. and AlSalloum, Y .A.(1995),"Flexural behavior of concrete elements reinforced by GFRP bars" Taerwe, L. (Ed.), Non-metallic FRP Reinforcement for concrete Structure, E&F Spon, London, pp.219-26.

[5] Benmokrane B., Chaallal O., and Masmoudi R. (1996), “Flexural Response of Concrete Beams Reinforced with FRP Reinforcing Bars,” ACI Structural Journal, Vol. 93, No. 1, Jan.-Feb. 1996, pp. 46-55.

[6] Brown V. L., and Bartholomew C. L. (1993), “FRP Reinforcing Bars in Reinforced Concrete Members,” ACI Materials Journal, Vol. 90, No. 1, Jan.-Feb 1993, pp.34-39.

[7] Favre R, Charif H. “Basic model and simplified calculations of deformations according to the CEB-FIP model code 1990”. ACI Stru. J 1994; 91(2):169–77.

[8] Ghali A, Hall. “Deflection of reinforced concrete members” a critical review. ACI Struct J 1993; 90(4): 364–73.

[9] Houssam A. Toutanji. H and M. saafi (2000),"Flexural behavior of concrete beams reinforced with Glass fiber reinforced polymer (GFRP) bars,"," ACI structural journal, V.97, No. 5, September – October 2000, pp. 712-719.

[10] ISIS Canada (2001), “Reinforcing Concrete Structures with Fibre Reinforced Polymers, Design Manual No. 3,” Intelligent Sensing for Innovative Structures, Manitoba, Canada.

[11] Leung, H. Y., Balendran, R. V. (2003)," Flexural behavior of concrete beams internally reinforced with GFRP rods and steel rebars" Structural survey J. 03) 21(4), pp. 146-157.

[12] Masmoudi R., Theriault,M., and Benmokrane B. (1998), “Flexural Behaviour of Concrete Beams Reinforced with Deformed Fiber Reinforced Plastic Reinforcing Rods,” ACI Structural Journal, Vol. 95, No. 6, Nov.-Dec. 1998, pp. 665-676.

[13] M. A. Aiello., L. Ombres. (2003)," A rational use of FRP rebars in designing of reinforced concrete flexural structures" 2nd conference on the conceptual approach to structural design, 1-2 July, 2003-Milan, Italy, pp. 201 – 208.

[14] Nawy, E. G., Neuwerth, G. E.,” fiber glass reinforced concrete slabs and beams”. Journal of the structural engineering division, ASCE, (1977) 421-440.

[15] Theriault M., and Benmokrane B. (1998), “Effects of FRP Reinforcement Ratio and Concrete Strength on Flexural Behaviour of Concrete Beams,” Journal of Composites for Construction, ASCE, Vol. 2, No. 1, Feb. 1998, pp. 7-16.

السلوك الإنشائي للكمرات الخرسانية المسلحة بأسياخ من الألياف الكربونية أو الأسياخ المختلطة

تعتبر الألياف الكربونية من المواد المستحدثة والتي تستخدم كبديل لصلب التسليح لما لها من مميزات إلا أن العناصر المسلحة بتلك الألياف تبدى نقص في متانتها وصلادتها. وللتحسين من الأداء الإنشائي لتلك العناصر تم استخدام التسليح المختلط (الألياف الكربونية وصلب التسليح معا) كتسليح رئيسي . ثمانية عشرة كمرة مسلحة بنسب مختلفة إما من (ألياف كربونية فقط أو مختلطة أو من صلب التسليح فقط) تم اختبارها تحت الانحناء لتعيين عدد وعرض ومسافات الشروخ وكذا الترخيم والانفعال الحادثين.
تم تحليل هذه الكمرات باستخدام بعض الصيغ المتاحة من الأعمال السابقة وتقدير قيمة الترخيم المقابل لكل حمل وكذا الترخيم وعرض الشروخ المقابل لحمل الانهيار. كما تم مقارنة ذلك بالنتائج المعملية التي تم الحصول عليها . و في نهاية البحث أعطيت أهم النتائج والتوصيات المستخلصة والتي لها قيمة عملية في هذا المجال.